Bulletin of the Maritime Institute

Gdańsk, 2001, 28, 2

KONSTANTIN A. KLEVANNY
Flood Protection Department of St. Petersburg Administration
MORZASCHITA, St. Petersburg, Russia

VALENTINA P. GUBAREVA, MOHAMMAD S.W. MOSTAMANDY, LIDIA B. OZEROVA
North-West Hydro-Meteorological Service, St. Petersburg, Russia

WATER LEVEL FORECASTS FOR THE EASTERN GULF OF FINLAND

Abstract

The paper presents results of development and verification of the automated water level forecasting system for the eastern part of the Gulf of Finland with advance time 36 hours, which is based on two-dimensional hydrodynamic model of the Baltic Sea BSM3. The model is driven by the regional high-resolution atmospheric model HIRLAM. Boundary conditions in the Danish Straits are received from a big scale model of the Baltic and North Seas (OPMODEL). The system works at the North-West Regional Administration of Hydro-Meteorological Service of Russia (NWHMS).

1. Introduction

In the Baltic Sea the most intensive water level oscillations occurs in the Eastern Gulf of Finland (EGF). Storm winds over the Baltic Sea are capable of driving big volumes of water into the shallow head of the Gulf of Finland. Development of an automated and reliable system for the prediction of water level oscillations is a current task for many objects located along the EGF. In the first place amongst them is St. Petersburg, whose low-lying regions, referring to its central historical parts, are subject to flooding. Floods cause significant economic and social damage to the City, sometimes leading to human victims. Forecasts of high water levels are also very important for the Leningrad Nuclear Power Station. On the other hand forecasts of low water levels are necessary for a successful operation of St. Petersburg port and new ports, which are now under construction in the EGF.

Flooding starts in St. Petersburg when water level exceeds 160 cm above Kronshtadt zero. When the water level exceeds 3 m flood, it is classified as a catastrophic one. There have been about 300 floods in the City's history and 3 of them were catastrophic. The maximum water level rise (421 cm) occurred 19 November 1824.

The last flood in the City was 30 November 1999 (as for 13.11.2001). Maximum water level in station Gorniy Institute in St. Petersburg was 262 cm at 4 h 35 min (Moscow time). That day water flooded embankments, basements of many buildings, boilers, pumping stations and machine rooms of some bridges. Water penetrated in the subway tunnel, and some stations were closed. Three ships were carried away from moorings. Some of St. Petersburg suburbs, located along the coast, suffered also. At night rescuers evacuated sleeping people, and among them children from one of the sanatoria. At 2 a.m. the Commission of Emergency situations headed by the Governor began its work. Radio translated the instructions of the Ministry of Emergency Situations, for the case of flooding; to turn off the electricity and gas, take warm clothes, documents, food for three days and to prepare for evacuation.

After the flood of 15 October 1955 (293 cm) and in connection with the work under the general plan of Leningrad development, the projection of St. Petersburg flood protection barrier in the Neva Bay was started. The construction began in 1979, but in 1990, when 60% of the work had been completed, the Leningrad City Council stopped the construction. This decision was based on the recommendation of the Commission on the ecological expertise of the Barrier of the Presidium of the Academy of Sciences of the USSR. In 1994 the Russian Government, after positive conclusions of the International Commission of experts, took the decision to complete the Barrier construction in 2001, but due to lack of finances the work continued very slowly.

Since 1990 there are parts of the Barrier that cannot close during flooding, the largest part being the navigation sluice, which is 940 m wide. According to simulations [1] these openings do not allow for protection against flooding in St. Petersburg. Therefore, at this present time, early forecasting of floods is necessary to give advance warning to the concerned services and the population. After completion of the Barrier, advance forecasts will be needed for the Barrier operation.

Forecast of water levels in the EGF is the official task of the North-West Regional Administration of Hydro-Meteorological Service of Russia (NWHMS). Until 1967 the forecasts were based on the empirical methods only [2,3]. Since 1967 and until 1997 in the case of threat of flooding the one-dimensional model of the Baltic Sea with advance time 12 hours was used as an additional tool. The model was developed at the Leningrad branch of the State Oceanographical Institute [4-6]. The model grid consisted of 200 points. In the early period the forecasted atmospheric pressure field was calculated with the methodology of Hydrometcentre [7] and later it was received from the European Centre in Bracknell with the space step 2.5° and the time step 12 hours. Root mean square error for station Gorniy Institute was 49 cm for hourly water levels during 51 floods (612 values) and 57 cm for the peak values of these floods. The main source of error was too big time step of meteorological data. Verification of the model with the measured pressures showed that the root mean square error was decreased to 31 cm for the hourly values (902 values) and to 29 cm for the peak values (69 floods) [6].

This paper presents results of the development and verification of a new fully automated flood forecasting system with the advance time 36 hours. The system is based on a two dimensional model of the Baltic Sea BSM3 and a high resolution regional model of the dynamics of atmosphere HIRLAM, which works in the operational regime at the Swedish Meteorological and Hydrological Institute (SMHI) in Norrköping. The water exchange between the Baltic and the North Seas is assigned according to forecasts made with a large scale model of the North and Baltic seas (OPMODEL), which works operationally at the Federal Agency for Navigation and Oceanography (Bundesamt für Seeschifffahrt und Hydrographie, BSH) in Hamburg.

BSM3 model was developed with the modelling system CARDINAL (Coastal ARea Dynamics INvestigation ALgorithm) CARDINAL is the user-friendly computer program for construction of regional models of arbitrary water objects and simulation of currents, water levels and dispersion of pollutants in 2D and 3D approaches [8-11].

The work was made basically in 1999-2000 with the financial support of the Netherlands Ministry of Economic Affairs (grant PSO98/RF/3/10). The authors express their gratitude to the project leader Herman Gerritsen of WL | Delft Hydraulics in The Netherlands, Hans Dahlin, Lennart Robertson and Michael Andersson of SMHI, Klaus Huber and Sylvin Müller-Navarra of BSH.

2. Model equations

For the simulation of long wave dynamics of the Baltic Sea 2D shallow water equations were used in the BSM3 model

$$U_t + gH\varsigma_x = -\left(\frac{U^2}{H}\right)_x - \left(\frac{UV}{H}\right)_y + C_D\frac{\rho_a}{\rho_0}w_{(x)}|\vec{W}| - \frac{H}{\rho_0}\frac{\partial P_a}{\partial x} - f_b\frac{U|\vec{V}|}{H^2} + fV + K\Delta U \quad (1)$$

$$V_t + gH\varsigma_y = -\left(\frac{UV}{H}\right)_x - \left(\frac{V^2}{H}\right)_y + C_D\frac{\rho_a}{\rho_0}w_{(y)}|\vec{W}| - \frac{H}{\rho_0}\frac{\partial P_a}{\partial y} - f_b\frac{V|\vec{V}|}{H^2} - fU + K\Delta V \quad (2)$$

$$\varsigma_t + U_x + V_y = 0 \quad (3)$$

where U, V are the components of the full flux vector $\vec{V}(x,y,t)$ in the x (east) and y (north) directions, g is the gravity acceleration, $H = h + \zeta$ is the full depth, $h(x,y)$ is the undisturbed depth, $\zeta(x,y,t)$ is water level, $C_D(W)$ is the wind drag coefficient, ρ_a is air density, ρ_0 is water density, $\vec{W}(x,y,t)$ is the wind vector with components $w_{(x)}$ and $w_{(y)}$, $P_a(x,y,t)$ is the surface pressure, f_b is the bottom friction coefficient, $f(y)$ is the Coriolis parameter, K is the coefficient of horizontal eddy viscosity and Δ is 2D Laplacian.

On the solid parts of lateral boundaries the following boundary conditions were assigned for the components of the flux vector

$$V_n = 0$$

$$K\frac{\partial V_\tau}{\partial n} = f_b\frac{V_\tau|\vec{V}|}{H} \quad (4)$$

where V_n and V_τ are the normal and the tangential to the boundary components of the flux vector, respectively. On the open part of lateral boundaries boundary conditions have the form

$$V_n = V_0(t)$$

$$K\frac{\partial V_\tau}{\partial n} = 0 \quad (5)$$

For the increase of accuracy of numerical solution of these equations they were transferred to the boundary-fitted curvilinear coordinates

$$\xi = \xi(x,y), \quad \eta = \eta(x,y) \quad (6)$$

with the Jacobian of transformation $J=(x_\xi y_\eta - x_\eta y_\xi)$, $0<J<\infty$. Along boundary line one of the coordinates is fixed and other one distributed arbitrary but monotonically. In some points change of the fixed coordinate is assigned. The Cartesian components of flux U, V were changed on the contravariant ones $(y_\eta U - x_\eta V)/J$ and $(x_\xi V - y_\xi U)/J$.

After some transformations equations (1) - (3) may be written in the form

$$P_t + \frac{gH}{J}(g_{22}\varsigma_\xi - g_{12}\varsigma_\eta) =$$
$$= -\frac{1}{J}\left\{\left(\frac{P^2}{H}\right)_\xi + \left(\frac{PQ}{H}\right)_\eta + \frac{y_\eta Q + y_\xi P}{JH}\left(x_{\xi\eta}P + x_{\eta\eta}Q\right) - \frac{x_\xi P + x_\eta Q}{JH}\left(y_{\xi\eta}P + y_{\eta\eta}Q\right)\right\} + \tag{7}$$
$$+ C_D\frac{\rho_a}{\rho_0}(y_\eta w_{(x)} - x_\eta w_{(y)})|\vec{W}| - \frac{H}{\rho_0}\left(y_\eta\frac{\partial P_a}{\partial x} - x_\eta\frac{\partial P_a}{\partial y}\right) - f_b\frac{P|\vec{V}|}{H^2} +$$
$$+ \frac{f}{J}(g_{22}Q + g_{12}P) + \frac{K}{J^2}[g_{11}P_{\eta\eta} + g_{22}P_{\xi\xi} - 2g_{12}P_{\eta\xi}]$$

$$Q_t + \frac{gH}{J}(g_{11}\varsigma_\eta - g_{12}\varsigma_\xi) =$$
$$= -\frac{1}{J}\left\{\left(\frac{Q^2}{H}\right)_\eta + \left(\frac{PQ}{H}\right)_\xi + \frac{x_\xi P + x_\eta Q}{JH}\left(y_{\xi\eta}Q + y_{\xi\xi}P\right) - \frac{y_\eta Q + y_\xi P}{JH}\left(x_{\xi\eta}Q + x_{\xi\xi}P\right)\right\} + \tag{8}$$
$$+ C_D\frac{\rho_a}{\rho_0}(x_\xi w_{(y)} - y_\xi w_{(x)})|\vec{W}| - \frac{H}{\rho_0}\left(x_\xi\frac{\partial P_a}{\partial y} - y_\xi\frac{\partial P_a}{\partial x}\right) - f_b\frac{Q|\vec{V}|}{H^2} -$$
$$- \frac{f}{J}(g_{11}P + g_{12}Q) + \frac{K}{J^2}[g_{11}Q_{\eta\eta} + g_{22}Q_{\xi\xi} - 2g_{12}Q_{\eta\xi}]$$

$$\varsigma_t + \frac{1}{J}\left(P_\xi + Q_\eta\right) = 0 \tag{9}$$

where $P = y_\eta U - x_\eta V$, $Q = x_\xi V - y_\xi U$ are the contravariant components of the full flux, multiplied on the Jacobian of transformation, which characterize water discharges, $g_{11} = x_\xi^2 + y_\xi^2$, $g_{22} = x_\eta^2 + y_\eta^2$ and $g_{12} = x_\eta x_\xi + y_\eta y_\xi$ are the components of covariant metric tensor, which characterize square of compression along the corresponding direction (the components with repeated index), and cosine between coordinates lines (the component with different indices). The later turns to zero for the orthogonal coordinates.

For the horizontal eddy viscosity terms, which are determined empirically and approximately a simplification was introduced in the curvilinear coordinates: terms with the second and the third derivatives of the metric coefficients were omitted. So, the next terms were omitted in (7)

$$-\frac{K}{J^2}[g_{22}(2y_{\eta\xi}U_\xi + y_{\eta\xi\xi}U + 2x_{\eta\xi}V_\xi + x_{\eta\xi\xi}V) + g_{11}(2y_{\eta\eta}U_\eta + y_{\eta\eta\eta}U + 2x_{\eta\eta}V_\eta + \tag{10}$$
$$+ x_{\eta\eta\eta}V) - 2g_{12}(y_{\eta\eta}U_\xi + y_{\eta\xi}U_\eta + y_{\eta\xi\xi}U + x_{\eta\eta\xi}V + x_{\eta\xi}V_\eta + x_{\eta\eta\xi}V)]$$

Boundary conditions (4) for the solid parts of lateral boundaries along lines $\eta = const$ took the form

$$Q\big|_{\eta = const} = 0; \quad K\frac{\sqrt{g_{11}}}{J}\frac{\partial P}{\partial \eta}\Big|_{\eta = const} = f_b\frac{P|\vec{V}|}{H} \tag{11}$$

Along $\xi = const$ lines conditions (4) took the form

$$P\Big|_{\xi=const}=0; \quad K\frac{\sqrt{g_{22}}}{J}\frac{\partial Q}{\partial \xi}\Big|_{\xi=const}=f_b\frac{Q|\vec{V}|}{H} \tag{12}$$

Conditions (5) for the open parts of lateral boundaries were transferred to

$$Q\Big|_{\eta=const}=Q_0(t); \quad \frac{\partial P}{\partial \eta}\Big|_{\eta=const}=0 \tag{13}$$

$$P\Big|_{\xi=const}=P_0(t); \quad \frac{\partial Q}{\partial \xi}\Big|_{\xi=const}=0 \tag{14}$$

For transfer to the curvilinear boundary fitted coordinates an algorithm is needed, which can map an arbitrary physical domain onto a canonical computational domain. One of such method is the elliptical one [12]. Coordinates $x(\xi\,\eta)$ and $y(\xi\,\eta)$ inside the area were found from the solution of the system of equations

$$g_{22}\,x_{\xi\xi}-2g_{12}\,x_{\xi\eta}+g_{11}\,x_{\eta\eta}=0 \tag{15}$$

$$g_{22}\,y_{\xi\xi}-2g_{12}\,y_{\xi\eta}+g_{11}\,y_{\eta\eta}=0 \tag{16}$$

with the Dirichlet boundary conditions: $x(\xi\,\eta)$ and $y(\xi\,\eta)$ are assigned along boundary coordinate lines ξ=*const* and η=*const*, which correspond to the outer boundary and islands, i.e. area may be multi-connected. Equations (15) and (16) are followed after conversion of variables in the Laplace equations

$$\xi_{xx}+\xi_{yy}=0; \quad \eta_{xx}+\eta_{yy}=0 \tag{17}$$

The elliptical systems allow assigning all two (or three in 3D case) coordinates on all boundaries and they possess the maximum principle. In elliptical system the coordinates $x(\xi\,\eta)$ and $y(\xi\,\eta)$ tend to distribute equidistantly as much as it allow the boundary conditions. The finite difference analogs of equations (15) and (16) can be solved iteratively with the upper relaxation method of Gauss - Seidel. The initial distribution of $x_0(\xi\,\eta)$ and $y_0(\xi\,\eta)$ is arbitrary.

3. Numerical method

Let us consider briefly the numerical procedure of solving the transformed shallow water equations (7) - (9). These equations were solved with the semi-implicit finite-difference method, in which the gravitational mode and the bottom friction were approximated implicitly, while advection, the Coriolis force and horizontal eddy viscosity were approximated explicitly. Fully staggered *C*-grid of Mesinger-Arakawa was used. The central differences were used for the space derivatives, and approximation of Crank-Nicholson was used for the time derivatives. The boundary of computational domain crosses *P*- and *Q*-points, and ζ-points were inside it. The equations were solved with the time-splitting method of the second order of accuracy.

The method of solution was the following. On the first half-step $\overset{*}{\varsigma}_{\xi}$ and P^* in the bottom friction term in (7) are taken from the upper time level (*). Other terms are approximated explicitly. Water level ζ^* on the upper time level in (7) is excluded using the mass conservation equation (9), where P^*_{ξ} is approximated implicitly. The implicit equation for the flux component P^* is solved with the three-diagonal solver. Then ζ^* and Q^* on the first half-step are found explicitly from (8) and (9). On the second half-step the similar procedure is used to find implicitly Q^{n+1} from (8) and (9) and then explicitly ζ^{n+1} and P^{n+1} from (7) and (9).

For the approximation of $g_{12}\zeta_\eta$ in (7) in the internal P-points 4-points central-space finite-difference stencil was used, but in P-points adjacent to boundary lines $\eta=const$, we have to use one-side differences directed into the computational domain. Therefore it is important to minimize values of metric coefficient g_{12} at the boundaries. For the approximation of the horizontal eddy viscosity terms near the boundaries extrapolation of fluxes components out of area is necessary. The boundary conditions (11) and (12) are used for this. Thus, for the approximation of $P_{\eta\eta}$ in P-points near $\eta=const$ boundary, P_0 outside the computational domain was calculated from

$$P_{i,0} = \frac{P_{i,2}}{1+\dfrac{f_b J}{KH\sqrt{g_{11}}}|\vec{V}|} \tag{18}$$

The spectral Fourier method showed, that if the right-hand side in (7) - (8) is omitted, the numerical scheme is absolutely stable and has no internal dissipation: all three eigenvalues of the transition matrix are equal to unity. In the general case due to the explicit approximation of terms in the right hand side, the scheme has limitations on the time step. Absence of the scheme viscosity is the positive feature of the scheme: solution does not dissipate due to numerical errors. High frequency oscillations, which appear due to the approximation errors, should be dampened with the dissipative terms $K\Delta U$, whose appearance in this scheme, generally, is necessary.

4. Baltic Sea model BSM3

Equations (7) - (9) with boundary conditions (11) - (14) were solved in the BSM3 model in the area, which corresponds to the Baltic Sea. With equations (15) and (16) the computational domain was mapped onto computational rectangular with a number of indents (Fig. 1). The total number of points was 60885 and among them 30894 were water points. Along the line "Stockholm – the head of the EGF" 205 grid points were assigned, and along the line "the Danish Straits – the head of the Gulf of Bothnia" - 297 points. Across the Gulf of Finland (from south to north) grid has 43 points and in the EGF – 29 points. Parts of the grid for the Baltic proper and for the head of the Gulf of Finland are shown in Figs. 2,3.

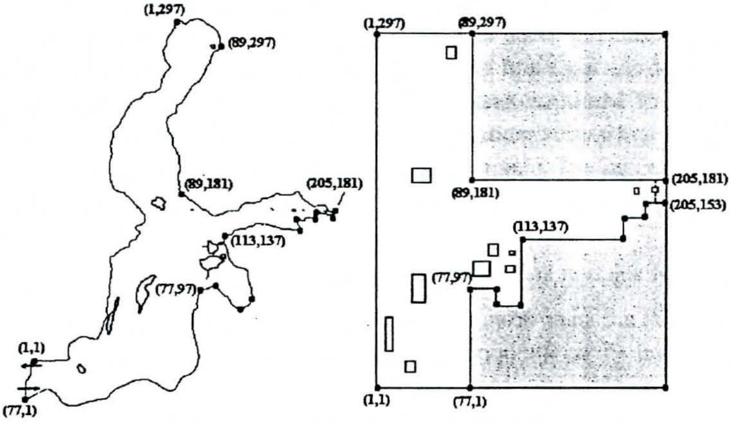

Fig. 1. Scheme of mapping of the Baltic Sea onto computational domain in the BSM3 model

St. Petersburg flood protection barrier, which has, at present, 9 openings, was approximated in the BSM3 by one dam with two openings at its edges in the South Gate of the Neva Bay and by two dams with openings between them and near the north shore in the North Gate (Fig. 3). Squares of openings correspond to the present situation at the Barrier: 10651 m^2 in the South Gate and 4281 m^2 in the North Gate. Grid steps varied from 270 m in the Barrier openings to 35 km near the Latvian coast with the mean step about 3 km. The time step was 5 minutes.

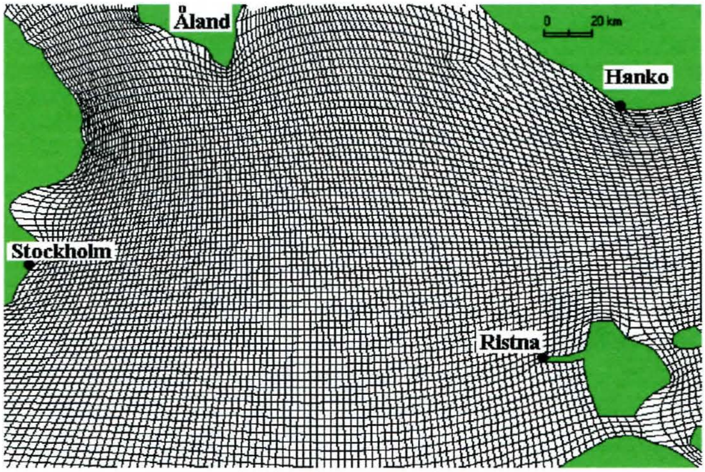

Fig. 2. Curvilinear grid for the central part of the Baltic Sea in the BSM3 model

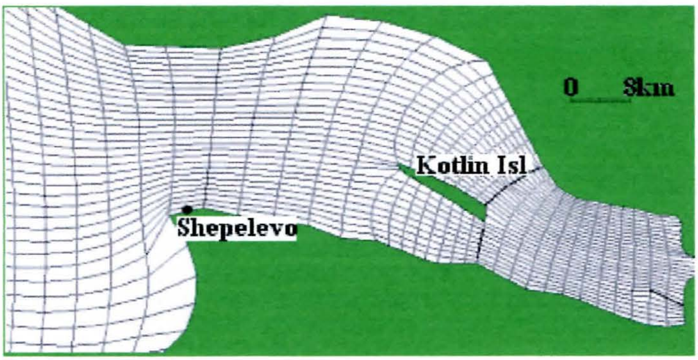

Fig. 3. Curvilinear grid for the Eastern Gulf of Finland and Neva Bay in the BSM3 model

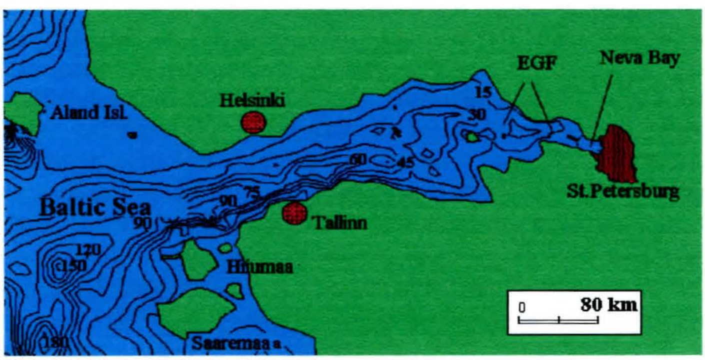

Fig. 4. Depth contours in the Gulf of Finland in the BSM3 model

Depths were assigned from the navigational maps. Initially depths were assigned in the nodes of rectangular grids. Grid steps were 20 km for the Baltic proper, 7.5 km for the Gulf of Finland and 2.5 km for the EGF and Neva Bay. Depth values in the nodes of the curvilinear grid were received with the linear interpolation from the rectangular grids. Usage of the navigational maps introduces, as is known, considerable errors in the hydrodynamic models, as these maps show all shallows, which are the most important for navigation. However, other sources of bathymetric data were not available. Depth contours for the Gulf of Finland in the model are shown in Fig. 4.

The bottom friction coefficient f_b was equal to 0.0026, the horizontal eddy viscosity coefficient K was equal to 1200 m^2/s. Calculations showed that variation of these parameters in a rather wide range did not have an influence on the results.

5. Organization of the system work

Since 27.10.1999 the forecasted fields of wind (10 m above the see level) and the surface atmospheric pressure have been received for the BSM3 model from SMHI. The High Resolution Local Area Model HIRLAM calculates at SMHI different meteorological parameters with the advance time 36 hours. The computational domain of HIRLAM covers the area with corners at 1) 30°N, 21°W, 2) 76°N, 42°W, 3) 65°N, 58°E, 4) 43°N, 23°E. This area includes a part of the North Atlantic, Greenland, Norwegian, North and Baltic Seas and a large part of Europe. Boundary conditions for HIRLAM are received from the global weather forecasts, which are produced at the European Centre for Medium Weather Forecast in Reading. Grid step in HIRLAM equals to 1/5° or 22 km. The grid consists of 713124 points (162 x 142 points in one horizontal layer, with 31 vertical layers).

Each HIRLAM output file contains data on 20 meteorological parameters for a certain time moment. These files are rather big (about 2.5 Mb); therefore SMHI produces special files for BSM3, which contain only surface wind and pressure, which are necessary for the system work. These files are loaded automatically on the FTP server of SMHI. Their size is 111 KB.

The HIRLAM data are transferred in packed GRIB (Gridded Binary) format, which is the WMO standard for transferring of big volumes of meteorological data. Data are packed in a way, that a minimum number of bits are used to represent values with a given accuracy. At first, the minimum value R is rejected from all data and then two scaling transformations of values are used. Initial value Y can be found from

$$Y = \frac{R + X \cdot 2^E}{10^D} \tag{19}$$

where X is the internal value, E is the power of the binary scaling and D is the power of the decimal scaling. This packing method allows transferring value of wind or pressure in 13 bits with the accuracy 7 significant digits. Usage of the standard methods would increase the volume of data in 2.5 times (32 bits per value). The GRIB file can contain any number of records, each of them contains values of a certain meteorological parameter. Each record has 3 - 5 sections: name of the section, section of data type determination, section with the grid definitions (optional), map section (optional) and the binary data section. For the work with GRIB data a decoder and special graphical procedures were introduced in CARDINAL. Detailed information of the GRIB format can be found at http://info.knmi.nl/wmow/doc/atlas/grib/gribma.

HIRLAM uses rotated latitude-longitude grid with the pole located in 30°S, 8°W. For transferring to ordinary coordinates, the next relations are used:

$$\sin\varphi' = \cos(\varphi_0 + \pi/2)\sin\varphi - \sin(\varphi_0 + \pi/2)\cos\varphi\cos(\lambda - \lambda_0)$$
$$\cos\lambda' = \frac{\cos(\varphi_0 + \pi/2)\cos\varphi\cos(\lambda - \lambda_0) + \sin(\varphi_0 + \pi/2)\sin\varphi}{\cos\varphi'} \quad (20)$$

where (φ_0, λ_0) are latitude $(-\pi/2 \le \varphi_0 \le \pi/2)$ and the eastern longitude $(0 \le \lambda_0 \le 2\pi)$ of the pole in coordinate system (φ, λ) expressed in coordinate system (φ', λ'). An example of decoded HIRLAM wind and pressure fields is given in Fig. 5.

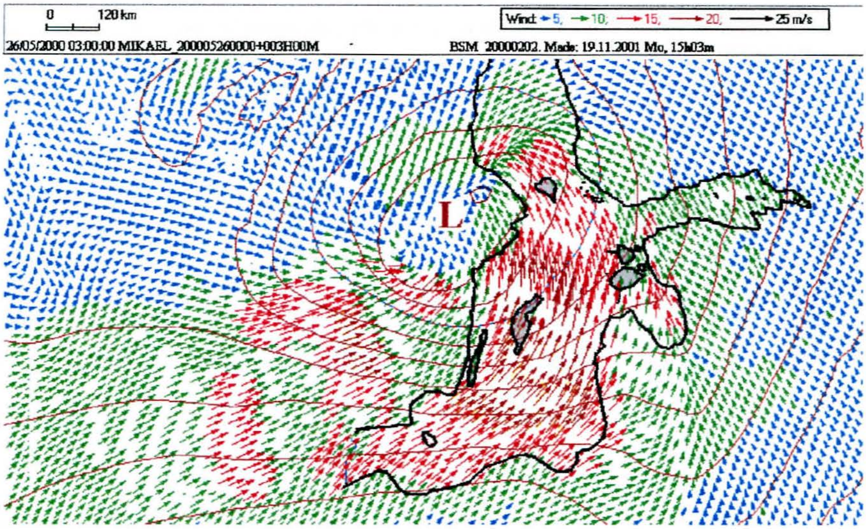

Fig. 5. Fragment of wind and surface pressure fields forecasted with the HIRLAM-22 model for 3 h UTC 26 May 2000. That day there was water level rise in the EGF (109 cm in Gorniy Institute at 18 h UTC)

Though HIRLAM output files are produced every day soon after 0 h UTC, but due to overloading of the SMHI computers, these files are loaded in the SMHI server only after 6 h UTC. Transferring of data to NWHMS is fully automated. Daily package consists of 13 files. The first one is forecast for 1 h a.m., the second - for 3 h a.m., the third – for 6 h a.m., and so on with the time step 3 hours. The last 13-th file is the forecast for 12 h a.m. of the next day. Due to the delay in data transferring, the actual advance of the forecast is reduced from 36 hours to 30 hours.

Wind in the BSM3 grid point is determined from the nearest HIRLAM point, and the pressure gradient is determined with the linear interpolation of values in four surrounding HIRLAM points. The linear interpolation is also used in time.

During the first stage of the system work, missing of the HIRLAM data took place. During the first half-year 10% of data had been missed. Unfortunately, data also had not been received during the only flood of 30 November 1999 of this period. At the present time missing of data occurs rarely.

Validation of the wind drag coefficient C_D, which has a very big influence on the results, was made using the HIRLAM data for November 1998 (data for November 1998 - July 1999 were received from the HIRLAM archive, also with 3 hours time step and 22 km space step). In November 1998 an anticyclonic circulation mainly characterized the weather over the Baltic and winds were not so high. During the period 21 - 23 November, however, the weather over the Baltic Sea was determined by the southern part of a deep cyclone. During these days there were strong southwestern winds over the Central Baltic and the Gulf of Finland.

As a result, there was a significant water level rise in the head of the Gulf. The HIRLAM wind velocities and the observed ones over the Baltic Sea were correlated well for this period. At the first approach, the wind drag coefficient was determined according to [13]:

$$C_D=(0.63+0.066|W|)\cdot 10^{-3} \quad (21)$$

During numerical experiments the second coefficient in (21) was varied until the simulated maximum of water level in Kronshtadt at the 22nd of November had become approximately equal to the observed value (101 cm). The best result (Fig. 6) was obtained with

$$C_D=(0.63+0.11|W|)\cdot 10^{-3} \quad (22)$$

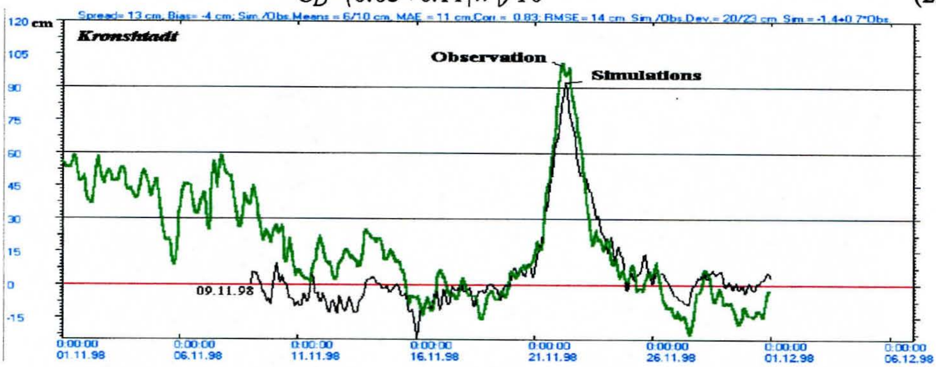

Fig. 6. Observed and simulated time history of water level in Kronshtadt in November 1998. $C_D=(0.63+0.11|W|)\cdot 10^{-3}$, zero initial water level. No water exchange through the Danish Straits, constant (2500 m^3/s) discharge of the Neva River

Value for the relation of air/water densities ρ_a/ρ_0 in (7), (8) was taken equal to $1.2\cdot 10^{-3}$. The root mean square error in this simulation was 14 cm, the mean absolute error - 11 cm, the correlation coefficient was 0.83. Relation (22) was used in all further simulations.

Since 03.12.2000 the system has been receiving forecasts of water exchange between the Baltic and North Seas through the Danish Straits. Studies of the Baltic Sea balance have shown that this water exchange is the main course of changes in the mean sea water level [14]. The forecasts are received daily from BSH in Hamburg, where simulations are made with the large-scale model of the North and Baltic Seas (OPMODEL). The results are received in the form of a text file. This file contains forecasts of discharges through the Great Belt, Little Belt and Øresund with the time step 15 minutes and with the advance time 4 days. Fig. 7 shows the time history of total discharges through three Danish Straits since 3.12.2000 and till 07.02.2001. Values of discharges sometimes exceed 250 thousand m^3/s. Their daily variability is connected with tides in the North Sea, while a long period changes reflect large-scale processes over the North Atlantic. The latter leads to significant seasonal oscillations of the Baltic Sea water level.

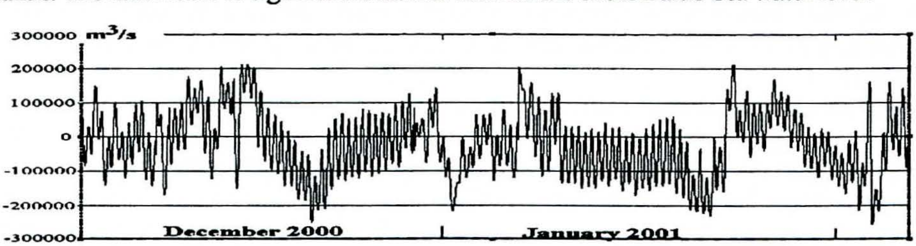

Fig. 7. The time history of discharges through the Danish Straits since 3.12.2000 and till 07.02.2001 forecasted at BSH. The positive values correspond to inflows into the Baltic Sea

Fig. 8 shows collated time history of changes to the water level in the Baltic Sea due to water exchange through the Danish Straits and the observed time history of water level in station Gorniy Institute for the same period of time. Changes of mean water level are obtained by dividing the total volumes of water, which have flowed through the Straits since 3.12.2000 in the area of the Baltic Sea, which was equal in the model to 346000 km^2. Since 3.12.2000 and till 7.02.2001 the volume of water in the Baltic Sea was decreasing due to water exchange with the North Sea on 133 km^3, which corresponds decreasing of mean water level on 38 cm. Comparison with the observed data for Gorniy Institute showed a good correlation of observed low water levels in the head of the Gulf of Finland in January - February 2001 with the simulated at BSH outflow of water in the North Sea.

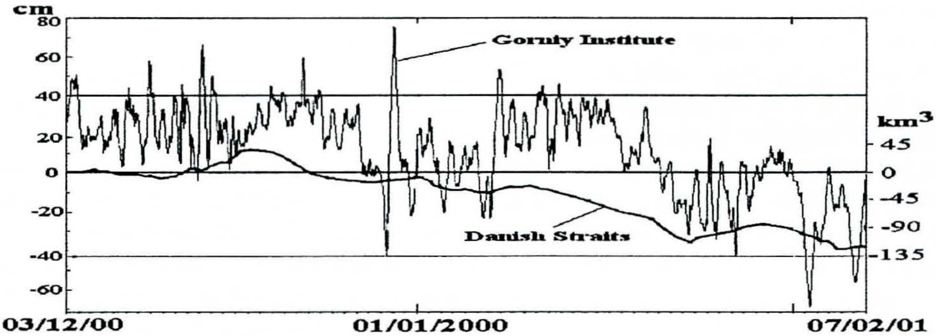

Fig. 8. Changes of the mean water level and water volume in the Baltic Sea due to water exchange through the Danish Straits forecasted at BSH and observed water level in Gorniy Institute since 3.12.2000 and till 7.02.2000

To take into account discharges through three Danish Straits, the model boundary was extended to the west and at present it goes along the narrowest cross sections of the Danish Straits.

Discharge of the Neva River was taken equal to 2500 m^3/s.

After forecasted data from SMHI and BSH are received, the Baltic Sea model BSM3 starts to run automatically. Simulations are made from 0 h UTC of the current day to the 12 h of the next day. Simulated fields of water levels and velocities, which correspond to 0 h of the next day are recorded and used as the initial data in simulations, which will be made on the next day. When simulations have finished, a one-page report is printed. At the present time this report contains forecasted time history of water level in Gorniy Institute in graphical and tabled forms, tables of forecasted winds and pressures over the EGF and Neva Bay, forecasted progressive-vector diagram of currents in the central part of the Neva Bay and forecasted change of mean water level in the Baltic Sea due to water exchange through the Danish Straits. The whole process of data receiving, simulations and printing of the result is fully automated. Simulations have been made at NWHMS since 23 December 1999. Pentium-III-500 computer is used. Simulation time is 10 minutes.

During the simulation it is possible to see, on a screen, different information in a graphical form: fields of wind, pressure, currents, water level in an arbitrary scale, the time history of water levels in any number of predetermined points. The time histories of water levels are saved and added to data received in previous simulations.

The experience received during a two-year validation of the developed system has proved that used methodology of data receiving and processing has robust character and is simple in use. The problem of missing meteorological data still remains.

6. Analysis of results

Figs. 9-21 show a comparison of forecasted and observed water levels in Gorniy Institute since December 1999 and until December 2000. The root mean square error of hourly data for this period (about 9000 values) equals to 20 cm, the mean absolute error is 16 cm, and the correlation coefficient is 0.73. The results are rather good. It should be noted that as water exchange through the Danish Straits have only been taken into account since December 2000, so before that, the mean water level of the sea was corrected manually, several times. There were no floods during this validation period.

A comparative analysis of forecasted and observed meteorological situations and water levels was made for 13 cases of significant water level rise. The analysis was hampered by lack of observed wind data.

1) 1.02.2000. According to the classification, which is used at the Hydro-Meteorological Service, the forecast of this water level rise (Fig. 11) is correct. That day, over the head of the Gulf of Finland, were the southwest winds up to 12 m/s and a primary cold front crossed the Gulf from the northwest. Forecasted wind fields coincide well with the observed ones.

2) 2.02.2000. There was a forecast of water level rise, but actually there was a decrease of water level (Fig. 11). With weak easterly winds in the head of the Gulf of Finland, an increase of water level was forecasted due to the long wave, formed near the Gulf entrance (the wave type of water level rise). This increase of water level at the Gulf entrance was forecasted as a result of strong southwest winds over the central Baltic. Though the pressure fields coincided in general, turn of wind in the head of the Gulf of Finland in reality was on 170° (from 210° to 40°), but not on 90° (from 180° to 90°). It is possible, that wind over the Baltic was weaker than it was forecasted.

3) 4.02.2000. Forecast of this water level rise was fully correct (Fig.11). Forecasted wind directions and velocities also coincided with the observed ones. The rise was connected with the increase of wind speeds at the cold front, which passed the Gulf of Finland from the west.

4) 6.02.2000. Forecast of this rise was correct in time, but forecasted water level was too high (Fig. 11). This rise was expected as a response of the wind turn from the southeast to the southwest during the passage of the cold front. Actually, this turn has occurred (on 50° from 210° to 260°) and it is possible that the forecasted wind speed over the eastern part of the Gulf (up to 15 m/s) was overestimated. Only data for Vyborg are available, where wind velocity was 7-10 m/s (15-17 m/s in gusts). But it is known that during the southwest winds Vyborg meteorological station overestimated winds.

5) 4.03.2000. Height of water level was underestimated (100 cm instead 132 cm, Fig. 12). Water level rise had occurred when the wind over the Neva Bay turned from150°-180° to 230°-240° and increased from 5 to13 m/s (up to 21 m/s in gusts). According to forecast wind should turn from 150° only to 170°-180° with speeds 6-8 m/s. This may cause underestimation of water level.

6) 12.03.2000. This forecast was correct (Fig. 12). The rise was connected with the passage of the secondary cold front over the head of the Gulf of Finland from the northwest. Forecasted and observed winds were the same in direction: 270-300°. Forecasted wind speeds over the EGF were 3-9 m/s, observed in Vyborg 4-7 m/s (13 m/s in gusts). The forecasted wind speeds over the Neva Bay were 3-4 m/s, observed ones lie mainly in the range 2-10 m/s (14 m/s in gusts).

7) 16.03.2000. A water level rise was predicted, but actually there was stable water level (Fig. 12). A complex wind field was forecasted. It was connected with a cyclone centre located to the south of the Neva Bay. Over the Neva Bay mainly weak winds of eastern directions were

forecasted. Water level rise was expected due to strong (up to 14 m/s) northwesterly winds over the central parts of the Gulf of Finland. Observed wind over the Neva Bay remains of the eastern direction. Over the Gulf of Finland it was closer to the north, and probably, it was weaker than the forecasted wind.

8) 6.04.2000. Forecast of the first water level rise (at 3 h a.m.) was correct in time and in maximum water level (Fig. 13). This rise was connected with the passage of the cold front and with turn of wind over the Neva Bay from 170° to 310°. This turn of wind was forecasted (with some delay in phase). Forecast of the second rise (at 3 h p.m.) was practically correct. This one was connected with the passage of the secondary cold front with the western wind 5-11 m/s. Approximately the same wind was forecasted.

9) 13.04.2000. Forecast was correct in time and in maximum water level (Fig. 13). This rise was connected with turn of wind from the east to the southwest after the passage of the warm front. The long wave was formed in the Gulf of Finland. The turn of wind was forecasted correctly.

10) 26.05.2000. Forecast was correct in maximum water level (Fig. 14). It may be noted that according to the forecast and observations, there were two peaks, but the forecasted maximum peak was the first one, while observations showed that maximum was the second one. The first peak (about 3 h p.m.) was connected with the passage of the cold front, and the second one (after 6 hours) was connected with the secondary cold front. In the whole, turn of wind from the southeast to the southwest and its increase was forecasted correctly. Forecasted weather situation at 3 h a.m. 26.05.2000 is shown in Fig. 5.

11) 3.06.2000. Forecasted maximum was underestimated, but the time of maximum was forecasted correctly (Fig. 15). The peak was connected with the passage of the cold front across the Gulf of Finland. Actual turn of wind was 90° (from the south to the west), but forecasted turn was 45° (from the south to the southwest).

12) 4.06.2000. Forecasted maximum was underestimated, but the time of maximum was forecasted correctly (Fig. 15). The peak was connected with the passage of the secondary cold front across the Gulf of Finland, turn of wind to the west and its sharp increase. This increase was forecasted correctly, but the forecasted wind direction was, as in the previous case, the southwestern.

13) 6.11.2000. Considerable underestimation of the maximum height (57 cm, observed value - 111 cm), the peak time was forecasted correctly (Fig. 20). The raise was connected with the passage of the cold front across the Gulf of Finland from the west. Forecasted wind coincides in general with the observed one in velocities and directions, but actual wind was closer to the west (Fig. 22).

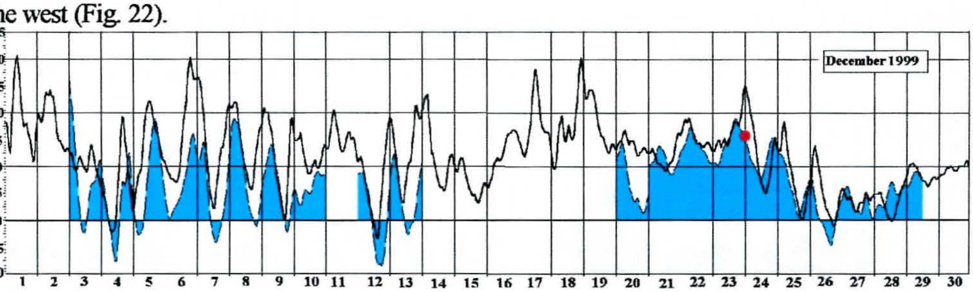

Fig. 9. Observed (thick line) and forecasted (thin line) time history of water level in Gorniy Institute in December 1999

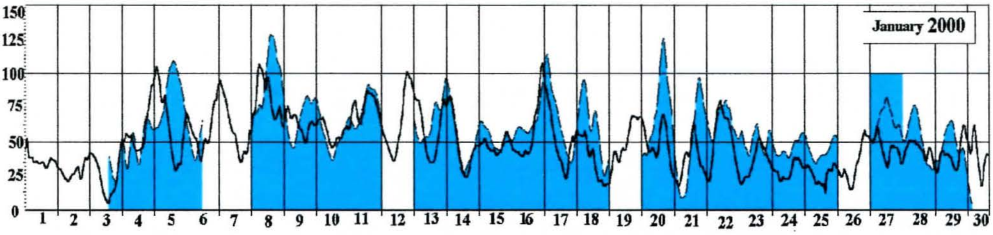

Fig. 10. Observed and forecasted time history of water level in Gorniy Institute in January 2000

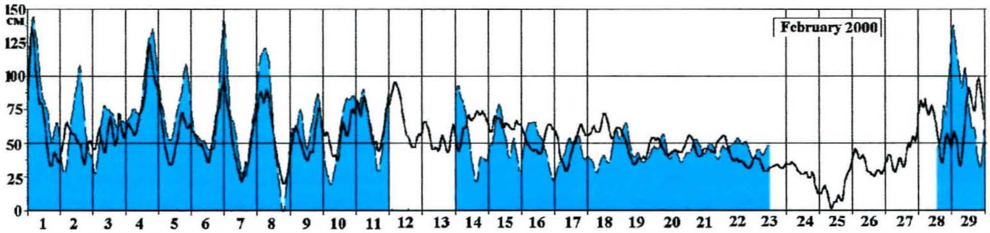

Fig. 11. Observed and forecasted time history of water level in Gorniy Institute in February 2000

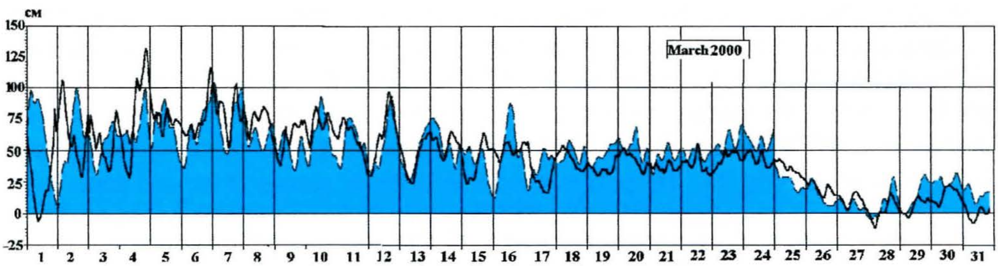

Fig. 12. Observed and forecasted time history of water level in Gorniy Institute in March 2000. Since 25 March the mean water level was decreased

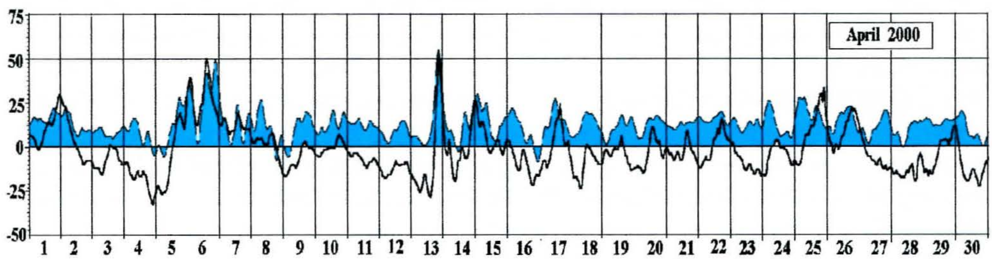

Fig. 13. Observed and forecasted time history of water level in Gorniy Institute in April 2000

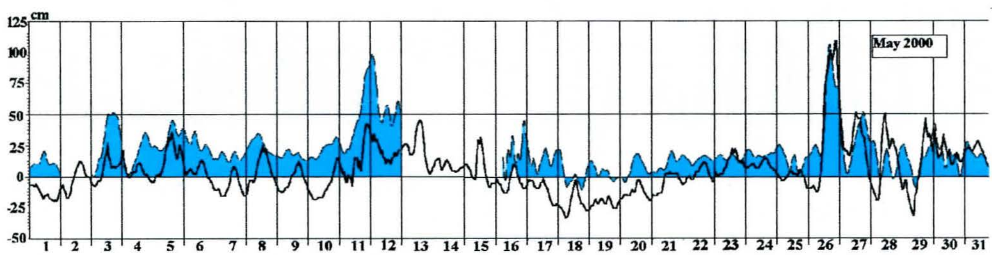

Fig. 14. Observed and forecasted time history of water level in Gorniy Institute in May 2000

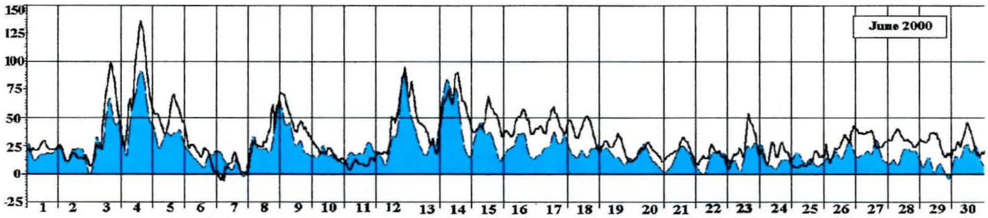

Fig. 15. Observed and forecasted time history of water level in Gorniy Institute in June 2000

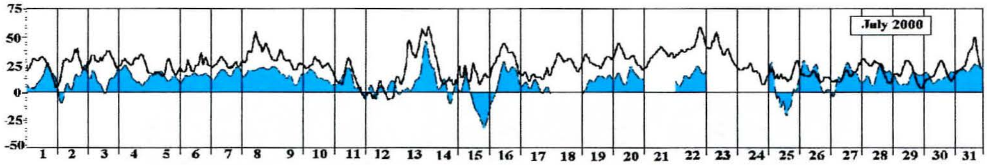

Fig. 16. Observed and forecasted time history of water level in Gorniy Institute in July 2000

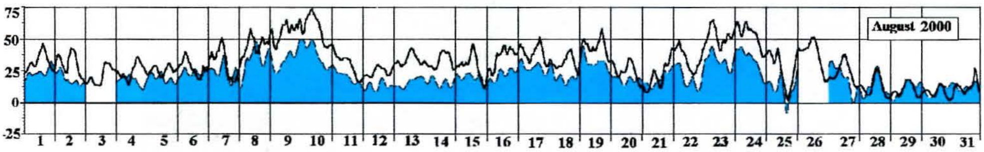

Fig. 17. Observed and forecasted time history of water level in Gorniy Institute in August 2000

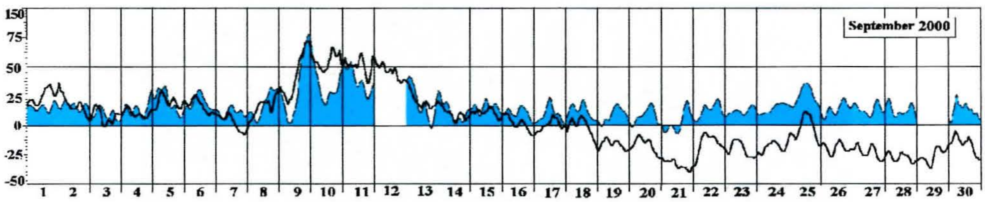

Fig. 18. Observed and forecasted time history of water level in Gorniy Institute in September 2000

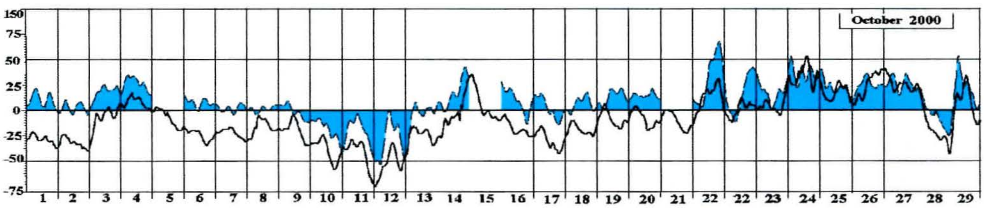

Fig. 19. Observed and forecasted time history of water level in Gorniy Institute in October 2000

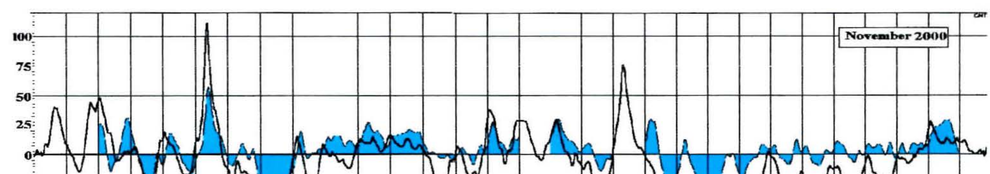

Fig. 20. Observed and forecasted time history of water level in Gorniy Institute in November 2000

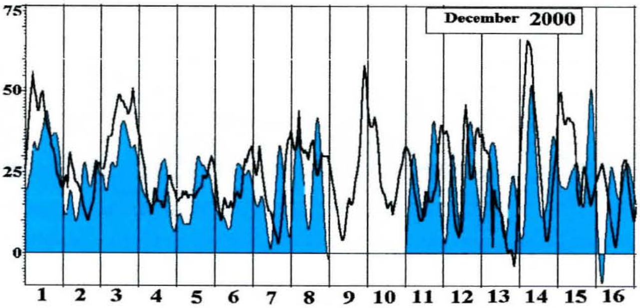

Fig. 21. Observed and forecasted time history of water level in Gorniy Institute 1-16 December 2000

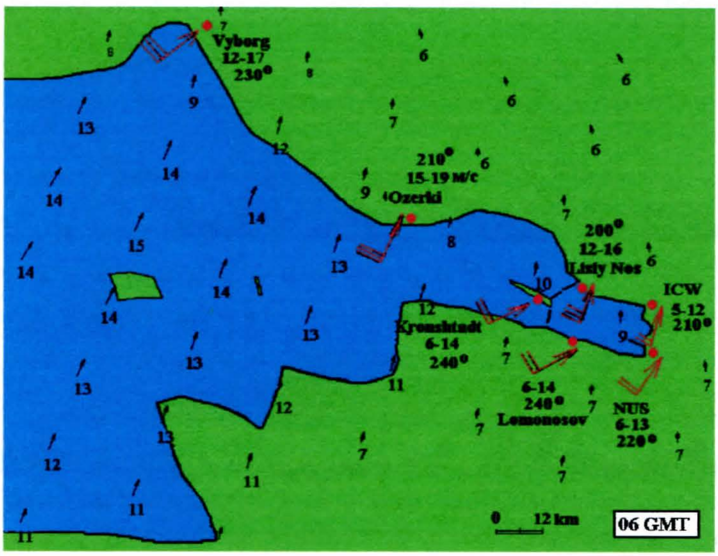

Fig. 22. Comparison of observed and forecasted winds over the EGF at 6 h UTC 6 November 2000. For the observed winds – the first values are mean velocities and the second ones are gusts. (NUS is the Neva mouth meteorological station, ICW is the Informative Weather Centre in St. Petersburg)

This analysis revealed that, as a rule, if wind field is forecasted correctly, then forecast of water level is also correct (cases 1, 3, 6, 8-10). The important source of errors in water levels is the errors in turn of wind over the Neva Bay: in cases 4 and 7 the maximum water levels were overestimated because actual turns of wind were less than the forecasted ones; in cases 11-13 the maximum water levels were underestimated as the actual turns of wind were bigger then the forecasted ones.

7. Conclusions

In conclusion it may be stated that the developed fully automated system of water level forecasts in the Eastern Gulf of Finland gives rather good results, better than all previous methods. There were no floods for the validation period considered and verification of the method will continue.

One of the sources of increase of the method accuracy is a more adequate description of atmosphere-sea interaction in the Baltic Sea model. It is necessary also to take into account ice cover for winter months and to include in the model the Neva River up to the Ladoga Lake (it will allow for forecasting the direction of the currents in the Neva delta). This work is in progress. After some tuning the system could be used for water level forecasts in other points of the Russian coast of the Baltic Sea (new ports of Primorsk, Ust'-Luga, Bukhta Batareinaya, Leningrad Nuclear Power Plant). It also may be used for forecasts of dispersion of pollutants and for operation of St. Petersburg Flood Protection Barrier.

References

[1] Klevanny K. A., 1999, *Protection of St. Petersburg against floods with uncompleted barrier: mathematical model study,* Proc. 5th International Conference on Coastal & Port Engineering in Developing Countries, Cape Town, South Africa, 62-637.

[2] Belski N. I., 1954, *Meteorological conditions of Leningrad floods,* Proc. of the State Oceanographical Institute 27, 39, 43-80. (In Russian).

[3] Freidson A. I., 1965, *Forecasting of the Neva Floods. Manual for the Short-Term Weather Forecasting*, part 3, 2, 8. (In Russian).

[4] Krugljak G. A., K. S. Pomeranets, R. V. Piaskovsky, E. N. Turuntaeva, 1982, *The catastrophic flood in Leningrad 23 September 1924 and its simulation,* Izv. All Union Geographical Society 1, 11-17. (In Russian).

[5] Piaskovsky R. V., K. S. Pomeranets, 1982, *Floods. Mathematical Theory and Forecasts*, Leningrad, Gidrometeoizdat Publ. (In Russian).

[6] Krugljak G. A., K. S. Pomeranets, R. V. Piaskovsky, 1984, *Accuracy of the hydrodynamic model of floods in Leningrad,* Probability analysis and modelling of oceanological processes. Leningrad, Hydrometeoizdat Publ., 159-163. (In Russian).

[7] Mertsalov A. N., 1964, *Forecast of surface pressure for 12-18 hours,* Collection of papers on regional synoptic 9, 3-39. (In Russian).

[8] Klevanny K. A., G. V. Matveyev, 1993, *CARDINAL User's Manual,* St Petersburg, Nevski Courier Publ.

[9] Klevanny K. A., G. V. Matveyev, N. E. Voltzinger, 1994, *An integrated modeling system for coastal area dynamics,* Int. J. for Numerical Methods in Fluids 19, 181-206.

[10] Klevanny K. A., G. V. Matveyev, 1995, *Integrated modeling system CARDINAL and its applications to estimation of environmental impacts of coastal engineering in the Gulf of Finland,* Proc. 4th International Conference on Coastal & Port Engineering in Developing Countries, Rio de Janeiro, Brazil, 3, 2120-2134.

[11] Klevanny K. A., 1999, *Modelling of long-wave processes in geophysical fluid dynamics,* Doctoral thesis. The Russian State Hydrometeorological University, St Petersburg. (In Russian).

[12] Thompson J. F., Z. U. A. Warsi, C. W. Mastin, 1982, *Boundary-fitted co-ordinate system for numerical solution of partial differential equation. A review,* J. Comp. Phys. 47 (2), 1-108.

[13] Smith S. D., E. G. Banke, 1975, *Variation of the sea-surface drag coefficient with wind speed,* Quart. J. Royal Meteorolog. Soc. 101, 429, 665-673.

[14] Gustafsson B., 1997, *Interaction between Baltic Sea and North Sea*, Deutsche Hydrographische Zeitschrift 49, 2/3, 165-183.